Simulation Studies of Diffusion-Limited Coarsening in Two Dimensions

Tang H. Wong and James A. O'Brien
Dept. of Chemical Engineering, Yale University, New Haven, CT 06520

The kinetics of particle coarsening are studied by means of contour dynamics simulation in two dimensions. The current method is free from the usual restrictions, such as small area fraction, constant particle shape, and local particle motion. Growth or shrinkage of particles in a given realization is found to depend on the local environment of the particles. The concept of critical size central to the classical theories such as the LSW theory, therefore, appears to be inappropriate. Surprisingly, the ensemble-averaged macroscopic behavior is consistent with mean-field theory. The particle-size distribution (PSD) tends toward an asymptotic shape, different from the mean field result. The normalized width of the PSD seems to be insensitive to volume fraction. Interfacial transport limitation can be significant for small particles, and it has the effect of altering the width of the PSD. The coarsening rate constant is found to be a function of the area fraction.

Introduction

Coarsening is a process by which particles, a discrete phase within a material, change their morphologies, with larger particles usually growing at the expense of smaller particles.The driving force behind these changes is the reduction of surface energy. If coarsening were allowed to proceed indefinitely, only a single particle would ultimately remain. At room temperatures, this process proceeds so slowly for most materials that no appreciable change can be observed even over a long period of time. At elevated temperatures such as those encountered during annealing or sintering, however, this process is very important in determining the morphology, and hence the physical properties of a material such as yield strength and hardness.

The coarsening rate is assumed to be diffusion-limited in most of this work, as in other work (e.g., Lifshitz and Slyovoz, 1961; Voorhees and Glicksman, 1984a,b) since diffusion through solid media, for example, is usually slow with respect to interface kinetic processes responsible for growth. (Generalization to reaction limitation will also be discussed.) This problem was first systematically studied by Ostwald in 1901 (Fischmeister and Grimvall, 1973) when he observed increased solubility of small particles compared to larger particles; hence, the phenomenon is also known as Ostwald ripening. The problem of grain growth by diffusion of solute in a matrix was treated first by Greenwood (1956). His analysis assumed that the interface between a particle and its immediate surroundings is at equilibrium, and the solute concentration at the interface can be described by the Gibbs-Thomson equation:

$$c_r = c \exp\left(\frac{2\gamma v_m}{R_g T r}\right) \tag{1}$$

where c_r is the solute concentration associated with a particle of radius r, c is the solute concentration in equilibrium with a particle of infinite radius (a flat surface), γ is the surface tension, v_m is the particle molar volume, and R_gT has the usual meaning. The particle was, of course, assumed to be spherical.

The cornerstone in the theoretical development was not laid until 1961 when Lifshitz and Slyozov and independently Wagner published their work which is collectively known as the LSW theory. The theory was based on the assumption that the mass flux to a particle of size R is given by

$$j = D\left.\frac{dc}{dr}\right|_{r=R} = D\frac{c_\infty - c_R}{R} \tag{2}$$

where D is the diffusion coefficient and c_R is the concentration at the surface of a particle. This idealizes the mass transport

---

Correspondence concerning this article should be addressed to J. A. O'Brien.

as occurring between the surface of an isolated sphere at equilibrium, and a source of constant concentration c_∞ an infinite distance away. Equation 2 is the solution of the quasi steady-state diffusion equation for this situation. The approximation leads to the correct qualitative behavior, in that particles smaller than some critical size shrink ($j<0$), while larger ones grow ($j>0$). Furthermore, it is implicitly assumed that interactions among particles can be neglected; this is strictly true only at very small volume fractions, where the separation between the particles is much larger than the size of any single particle. The essential result of the LSW theory is that the average volume of a particle scales linearly with time

$$\overline{R}^3 \propto t, \tag{3}$$

and the proportionality constant is known as the coarsening rate constant given by

$$k = \frac{4}{9} D\Gamma, \tag{4}$$

where $\Gamma = 2\gamma v_m / R_g T$ is the capillary length (Langer, 1980). In spite of the many subsequent criticisms of the theory, the scaling behavior, Eq. 3, appears to be indisputable. The major flaw of the theory, however, lies in the fact that the predicted particle-size distribution (PSD) is narrower and more skewed than that observed experimentally. Hence, one cannot reliably extract valuable information such as the surface tension and the diffusion coefficient from actual coarsening experiments. It is clear that when the volume fraction is small, the distance between particles, on the average, is large with respect to the particle size. Hence, because of the distance the solute has to diffuse, the rate of coarsening should decrease with decreasing volume fraction. For this reason, most of the modifications of the LSW theory have concentrated on the effect of volume fraction. The modifications usually account for the change in geometry of the diffusion field, which is affected by the volume fraction (Ardell, 1970; Davies et al., 1980; Marqusee and Ross, 1974). Due to the lack of information on the diffusion coefficient, it is difficult to compare experimental results against theoretical predictions. All of the modifications to the LSW theory predict an increase in the coarsening rate constant with increasing volume fraction, However, such effects are not always observed experimentally (Ardell, 1970; Chellman and Ardell, 1974); some experimental investigators have instead concluded that the rate constant is *independent of the volume fraction*. Despite this failure, all of the modified theories predict a broader particle-size distribution than that of the LSW theory, in qualitative accord with experiment.

The LSW theory assumes a mean-field approach: a particle responds not to the gradients of individual neighbors, but to an effective "smeared-out" field that is determined collectively by all of its neighbors. This assumption is expected to be locally valid at extremely low volume fraction. At higher volume fractions, however, it becomes a statistical concept arising from ensemble averaging, rather than an actual physical mean field.

In addition, the original LSW theory did not account for particle coalescence or actual physical impingement between particles. This phenomenon is usually assumed to be insignificant for low volume fraction systems, since the particles are so far apart that the chance of encounters is low. For high volume fraction systems, however, these mechanisms may be as important a factor as diffusion in determining the rate of coarsening. Davies et al. (1980), starting with the LSW theory, treated this problem and their theory is termed the Lifshitz-Slyozov encounter modified (LSEM) theory. This theory assumes that once the particles have coalesced, the resulting particle shape changes rapidly to the equilibrium shape by intraparticle diffusion. The rapid change is a result of the short distance over which solute has to diffuse since the exchanging sites are located in the same particle. A mechanism for particle coalescence proposed by Doherty (1982) models the event as a removal of the elastically-strained matrix between two parcles; hence, the process depends on the lattice mismatch. Similarly, elastic stress is not accounted for in the LSW theory. In fact, reverse behavior (smaller particles growing at the expense of larger particles) can even be predicted (Voorhees, 1990), if one considers a competition between ordinary and strain-induced concentration gradients.

Despite the past research efforts, a full picture of the process is still far from complete. The objective of this study is to test the validity or range of validity of the mean field approximation that forms the basis of many theories and to study the dependency of the coarsening rate constant on various factors such as volume fraction. In the next section, we describe a rather general, but powerful, technique to study the problem. This method was developed from the study of the interface dynamics (Brower et al., 1984; Wong and O'Brien, 1990), and it is sometimes referred to as contour dynamics. A similar method has been employed to study coarsening phenomena in two dimensions involving a smaller number of particles (McFadden et al., 1986; Voorhees et al., 1988). In this work, we also concentrate on the two-dimensional problem. The strength of this method is that all of the computational effort is directed at treating the development of the interface. It is, therefore, particularly suitable for handling particles of arbitrary shape, and those having anisotropy in various physical properties such as surface tension. Further, the method allows us to study systems not just in the limit of zero volume fraction, but at virtually any value. Although a similar study has been conducted by Voorhees and Glicksman (1984a,b), their approach is limited to spherical particles, and generalization to other geometries appears to be rather difficult. This is because they treated particles as points so that they could assign a single value for the concentration to each particle; however, particles at sufficiently high volume fraction (Ardell, 1970; Voorhees et al., 1988) are unlikely to remain spherical so that the method of Voorhees and Glicksman, which amounts to a first-order approximation, may suffer from accuracy problems. In addition, information on asymmetric particle growth, which occurs at all volume fractions, is missing from their method so that temporal variations in the local environment cannot be accurately tracked. As a consequence of representing particles as points their solution is strictly valid only for regions exterior to the particles. Our method is free from these restrictions. Currently, our method cannot handle particle coalescence; however, it appears that such phenomena could be handled by appealing to a related method known as contour surgery (see, e.g., Dritschel, 1989). The latter method extends the range of computation by removing small-scale features from the system, an idea which may be applicable to handling coalescence.

Of course, the major shortcoming of our approach is its restriction to two dimensions. While it is, in principle, possible to extend the methodology to three dimensions, the computational problems would probably not warrant the extraordinary effort involved. However, we can still learn qualitatively about the phenomena controlling coarsening by performing simulations in two dimensions. Further, a two-dimensional version of the LSW theory may be derived (Hillert, 1965), so that comparison between the simulation and a corresponding LSW-like analysis is still possible. In addition, there are physical situations that have previously been modeled by hemispherical particles interacting via two-dimensional diffusion fields, such as the coarsening behavior of metal particles on supported catalysts (Dadyburjor et al., 1986) and the grain-size evolution in thin films (Chakraverty, 1967).

It is commonly assumed (Voorhees and Glicksman, 1984a,b) that diffusion-limited coarsening is an equilibrium process in the sense that each particle's interface remains in equilibrium with its surroundings. While this is quite possible for the majority of the particles, its validity is far less clear for small particles. As a particle becomes smaller, the concentration difference between this particle and its neighbors increases; consequently, its interfacial velocity also increases. It is clear that the velocity cannot keep increasing indefinitely; hence, reaction limitation will eventually become important. We describe a technique to incorporate this phenomenon later.

Method

Particle interface velocity

The technique used here is an extension of our previous work (Wong and O'Brien, 1990); hence, only a brief description will be given here. The basic assumption is that the conserved field quantity, proportional to the concentration field, satisfies the quasisteady-state diffusion equation, Laplace's equation

$$\nabla^2\phi = 0. \tag{5}$$

Therefore, we are assuming a small Peclet number. The boundary of the system is insulated such that the conserved quantity is not allowed to pass through the boundary

$$\phi_n = 0, \tag{6}$$

where the subscript n denotes the gradient in the direction of the normal to the boundary. This boundary condition differs from that used by Voorhees et al. (1988), who employed an integral form of Eq. 6; ultimately, at the boundary of a coarsening system, one must demand that the flux *everywhere* approaches zero. However, the difference is not likely to be large in the cases considered here. Local thermodynamic equilibrium is assumed to exist at the surface of each particle: the interface between the particle and the matrix is given by the linear form of the Gibbs-Thomson equation

$$\phi|_{S_i} = 1 - \kappa\Gamma, \tag{7}$$

where κ is the local curvature and Γ is the capillary length (Langer, 1980). The general equation relating the interface concentration, ϕ, and its normal velocity, v, is

$$\frac{1+NB}{N+1}\phi = \overline{\phi_o} + \sum_{i=1}^{N}\oint_{S_i} Gv\,ds_i' + \frac{1-B}{N+1}\sum_{i=1}^{N}\oint_{S_i} G_n\phi\,ds_i', \tag{8}$$

where $B \equiv K_{\mathcal{R}}/K_{\text{particle}}$ is the ratio of the diffusivities for the outer matrix region $\mathcal{R}$ and the particles themselves, N is the total number of particles, v is the normal velocity of the interface (actually a collection of velocities of individual interfacial points) given by

$$v = -[\nabla\phi^+ - B\nabla\phi^-]\cdot\hat{\mathbf{n}}, \tag{9}$$

where $\nabla\phi^+$ and $\nabla\phi^-$ are the gradients of ϕ at the interface just outside and inside the particle, respectively, and $\overline{\phi_o}$ is the average value of ϕ at the outer boundary. Equation 8 is related to the equations presented by McFadden et al. (1986), who analyzed the problem in terms of potential theory, distributing monopoles and dipoles on the surfaces of the particles and adjusting coefficients to satisfy the boundary conditions. G is the Green's function (Dettman, 1988)

$$G(\mathbf{X}|\mathbf{Y}) = \frac{-1}{2\pi}\left[\ln(|\mathbf{X}-\mathbf{Y}|) + \ln\left(\left|\mathbf{X} - \frac{R_\infty^2}{|\mathbf{Y}|^2}\mathbf{Y}\right|\right) - \ln\left(\frac{R_\infty^3}{|\mathbf{Y}|}\right)\right], \tag{10}$$

where $\mathbf{X}$ is the source (field) point and $\mathbf{Y}$ is the field (source) point. One additional equation is needed to close the specification of the problem and it is supplied by conservation of material

$$\sum_{i=1}^{N}\oint_{S_i} v\,ds_i' = 0. \tag{11}$$

Because of the nature of the problem, the value of B is likely to be very close to unity. Therefore, we further assume that $B = 1$ in our simulations. With this assumption, Eq. 8 simplifies to

$$\phi = \overline{\phi_o} + \sum_{i=1}^{N}\oint_{S_i} Gv\,ds_i'. \tag{12}$$

By substituting Eq. 7 into Eq. 12 (or Eq. 8 for cases with B other than unity) and discretizing the interface of each particle into a number of segments, i.e., linearizing the set of integral equations, the velocity v can be obtained by solving the resulting set of linear equations [see Wong and O'Brien (1990) for more detail]. As pointed out earlier, we solve only for the quantities at the interface, since the interface completely quantifies the particle. The concentration field within the whole system, however, can be reconstructed by evaluating the Green's function at the desired position and substituting the known interface velocities into Eq. 12. This is a separate step that is completely decoupled from the main part of the calculation.

Interface evolution

The method for calculating the interface velocity is described in the previous section. The evolution of the interface can be calculated fairly straightforwardly from the velocity. A detailed description of the evolution equations can be found elsewhere (Wong, 1991). The interface can be described completely by two variables, for which we have chosen s_T, the total arclength of each particle and θ, the angle between the outward normal to the particle and the y-axis at each discrete interfacial point. Even though the interface is completely parameterized by θ and s_T, these quantities are inconvenient to use in the Green's function evaluation, which is best peformed with Cartesian coordinates. The location of the interface in Cartesian coordinates can be recovered by the following relations

$$x(s) = x_o + \int_0^s \cos\theta \, ds', \tag{13a}$$

$$y(s) = y_o - \int_0^s \sin\theta \, ds', \tag{13b}$$

where x_o and y_o correspond to the point where $s = 0$, the arbitrarily chosen beginning of the interface. Unlike our previous work with a single particle (Wong and O'Brien, 1990), evolution of the interface of a particle is no longer isotropic with respect to its center, and the apparent motion of a particle resulting from uneven growth at opposite sides must be accounted for. The complete set of evolution equations for each particle is

$$\dot{s}_T = \int_0^{s_T} \kappa v \, ds, \tag{14a}$$

$$\dot{\theta}\,|_\alpha = -\frac{\partial v}{\partial s} + s_T\kappa\left(\alpha\int_0^1 \kappa v\, d\alpha' - \int_0^\alpha \kappa v \, d\alpha'\right), \tag{14b}$$

$$\dot{x}_o = v|_{s=0}\cos\theta_o, \tag{14c}$$

$$\dot{y}_o = v|_{s=0}\sin\theta_o, \tag{14d}$$

where $\alpha = s/s_T$ (fractional arclength) and θ_o is the value of θ at $s = 0$.

Implementation and Simulation Details

According to the LSW theory, any particle-size distribution will eventually assume the "self-preserving" shape that is skewed toward larger particles, giving larger particles more influence on the average size. On the other hand, experimental PSD's are almost always broader and more symmetric than those predicted by the theory. Hence, it is of interest to track the development of the PSD. The initial PSD was chosen for the simulations to be fairly narrow and skewed toward smaller particles to exaggerate the evolution of the PSD. In this way, the PSD would not be "trapped" in a preconceived shape, if there were more than one possibility. The initial positions of the particles were chosen by a random scheme (random sequential placement of the particles in the plane) and a number of simulations (usually five) with the same initial PSD, but differently positioned particles were carried out to obtain an ensemble average. The highest initial volume fraction that could be achieved would be about 0.6 with this numerical scheme due to the fact that the distribution was fairly narrow; higher volume fractions can be achieved with wider distributions. However, the actual volume fractions used in the simulations were always lower than 0.6.

It has already been mentioned that local equilibrium at the particle interface is assumed (see below for nonequilibrium interface) so that the particle interfacial concentration can be approximated by the Gibbs-Thomson equation (Eq. 7). The interface velocity is related to the interfacial concentration through Eq. 8. In this study, we chose B to be unity based on the fact that the diffusion coefficients in the matrix and in the particles are unlikely to be very different.

A system of linear equations relating the interface velocity and the corresponding concentrations is obtained by discretizing the interface into a number of points and substituting Eq. 7 into the lefthand side of Eq. 12. Note that discretization of the interface linearizes the integral in Eq. 12. It is unfortunate that straightforward implementation of the Green's function is impossible because of the singularity when the source point and the field point coincide. The technique for handling this difficulty can be found in our previous work (Wong and O'Brien, 1990; Wong, 1991) and will not be repeated here. The essence of the technique is to carry out the integration analytically near the singularity by assuming a linear interpolation of the velocity in that region. This technique has proved to be accurate even with only a small number of discretization points. The set of nonlinear evolution equations (Eq. 14) is integrated by LSODA (Petzold, 1983). The advantage of LSODA over previous versions (e.g., LOSDE) is that depending on the linearity of the system, the Jacobian matrix is not calculated every time, and since Jacobian evaluations constitute a large portion of the total computation time, considerable savings can be achieved frequently.

The computational effort is related to the number of particles and the number of discretization points associated with each particle. All of the simulations reported here were performed with systems consisting of 65 particles and with eight discretization points per particle. The number of particles and discretization points was chosen based on a tradeoff between computational cost (favoring fewer particles) and good statistics (favoring more particles). Simulations have been carried out with more discretization points per particle than those reported here. However, the difference in the results was too small to justify the substantial increase in cost, since the computation time scales approximately as the cube of the number of equations (the number of particles times the number of discretization points per particle).

According to the Gibbs-Thomson equation, the interfacial concentration increases indefinitely as a particle shrinks. Hence, the concentration difference and, consequently, the mass flux, between a shrinking particle and its neighbors will also increase indefinitely. It is obvious that, at some point, the shrinkage rate will reach a maximum that is determined by the "reaction" or interfacial transport occurring at the surface of the particles. The process, therefore, becomes locally reaction-limited under this condition: the particle interface is no longer in equilibrium with its surroundings. It has been shown [see, for example, Wong and O'Brien (1990) and references therein] that if the interface deviates from equilibrium, the interfacial concentration can be approximated as (c.f. Eq. 7):

$$\phi = 1 - \Gamma\kappa - \beta v. \qquad (15)$$

where v is again the interface velocity and β is a kinetic parameter, reflecting the significance of the reaction limitation with respect to diffusion: $\beta \rightarrow 0$ for systems at equilibrium and $\beta \rightarrow \infty$ for reaction-limited systems. Note that even though the reaction limitation term applies to every particle, particles with higher velocities (usually smaller particles since they see higher gradients) are affected more than others. The effect of reaction limitation diminishes with increasing particle size (see Cahn, 1967; Wong and O'Brien, 1990). As shown in the Appendix, a typical value for β, based on an order-of-magnitude estimation, is ~ 100 for the dimensionless "sizes" we have chosen.

During the course of a simulation, the step size used by the integrator decreases when one of the particles is substantially smaller than the others. This is because the stiffness of the system, which is determined by the range of the interfacial velocities, increases as soon as one of the particles is substantially smaller than the rest. Hence, the velocity of the smallest particle becomes the dominant factor in determining the step size, which in turn controls the overall speed of the integration. This behavior should not affect the accuracy of the integration, since the integrator we used, LSODA, has the ability to adjust the step size. Thus, the scenario of particles with negative radii will never happen (although it will happen to integrators with a fixed step size (see also Voorhees and Glicksman, 1984a). It does, however, slow things down considerably. This increase in stiffness, therefore, motivates the introduction of a lower cutoff particle size. Particles that become smaller than this cutoff size are removed from the simulation. The cutoff size was chosen based on the observation that particles with sizes smaller than 10% of the mean size were rarely either reported in the literature or used in previous calculations. Even though the cutoff size may still appear to be large, the area at that size is only 1% of that of the mean particle area and approximately 0.25% of that of the largest particle. The loss in mass (area) associated with this removal is, therefore, roughly of the order 0.01%.

Results and Discussion

Mean-field assumption

The essence of the mean-field approximation is that a particle responds not to individual neighbors but to a "smeared-out" field determined by an ensemble average over the whole system. From a different viewpoint, the mean-field approximation at vanishing volume fractions assumes that the concentration gradient near a particle decays to the mean field before reaching another nearby particle. With reference to the evolution of the concentration field in our simulations, as shown in Figure 1, it would appear that the volume fraction (about 6%) is not small in this context. One can identify an *initial* mean field in Figure 1, since a narrow initial particle-size distribution was used as described in the previous section. As the system evolves,

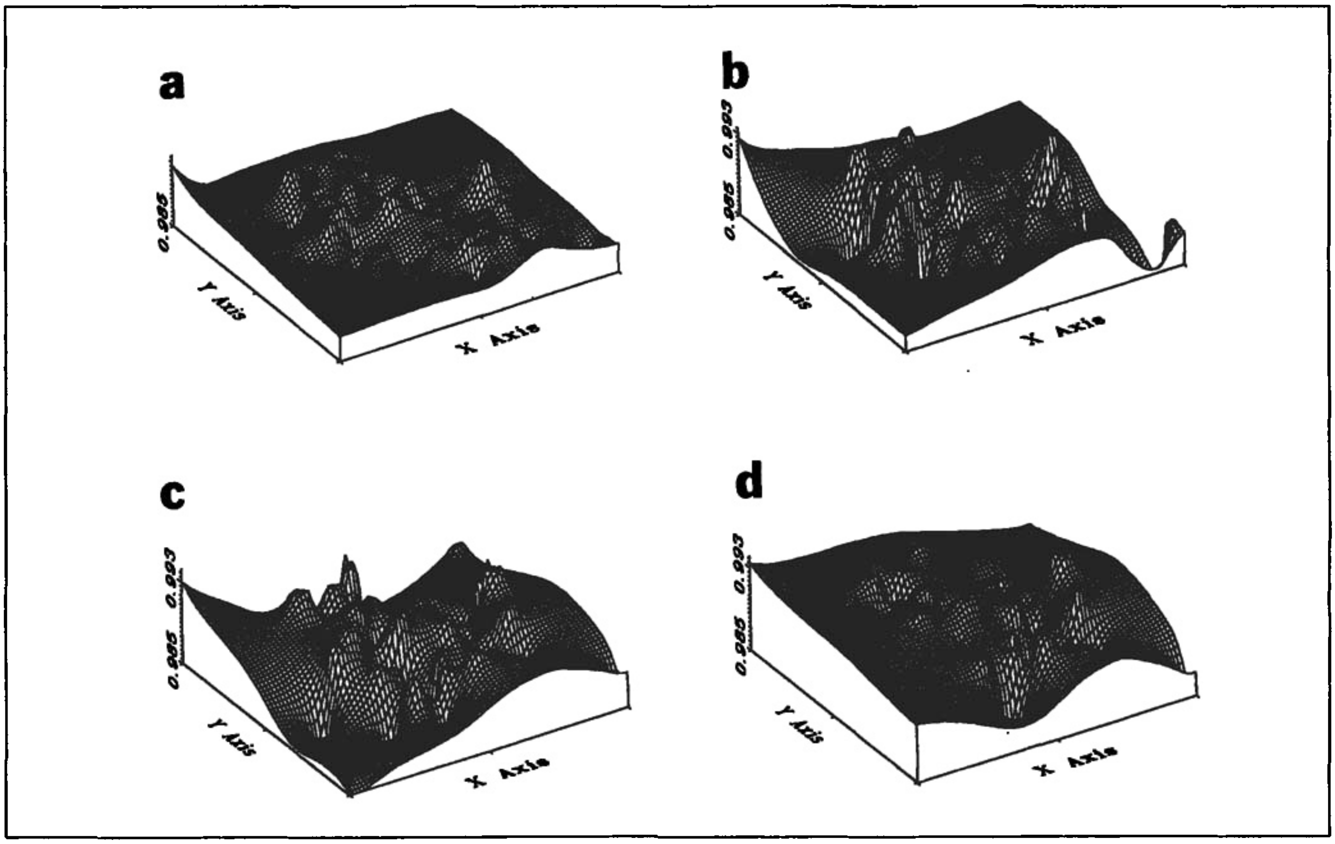

Figure 1. Evolution of the concentration field: area fraction = 0.06.

The initial distribution is given in (a) and the distributions at three successive times are given by the other three plots (c-d).

however, huge concentration gradients are developed between shrinking particles and their neighbors. It is clear that no local mean-field concentration can be identified under these conditions; hence, the mean-field approximation, which forms the basis of many theories, is demonstrated to be statistical in nature. This is in accord with the description of Voorhees and Glicksman (1984b). It should be pointed out that one could scale the vertical axis to "flatten" the distribution. Once the scale is fixed, however, the formation of steep gradients with time can still be seen, indicating that the behavior is genuine. While the particle concentration in Figure 1 is not exactly zero, the same conclusion nevertheless applies to the case of almost zero area fraction (Figure 2). Thus, the growth or shrinkage of particles depends on their local environments, where no *actual* mean field may be identified.

According to the LSW theory, particles with the same sizes should behave identically. Furthermore, it defines a time-dependent critical particle size such that particles with sizes smaller than the critical size will shrink and larger ones will grow. Lifshitz and Slyozov (1961) stated, "The motion (the growth or shrinkage of particles) is regular throughout in the sense that the initial order of a set of points is preserved." In other words, if particle x is smaller than particle y at some instant in time, then it is so for all time. With reference to Figure 3, the particles labeled A and B have the same initial size so that one would expect them to behave the same. On the contrary, particle A grows, while particle B shrinks. In view of this, it can be concluded that the critical size used in the theories does not actually exist in reality. In addition, the ordering of the particles is, therefore, also disturbed (see also Voorhees and

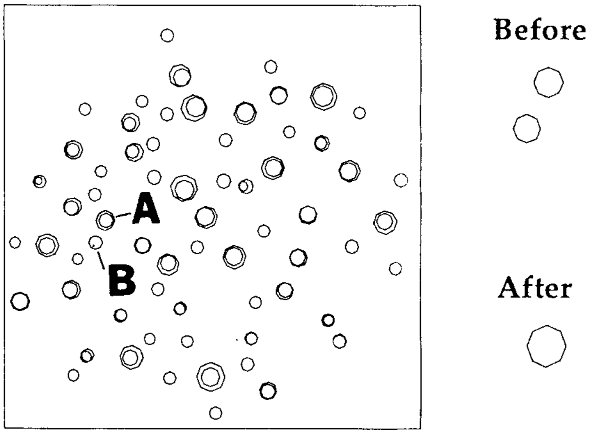

Figure 3. Evolution of the particle size: area fraction = 0.06.

Particles A and B have the same initial size. Particle A grows, while particle B shrinks. The enlarged initial and final sizes of the particles are shown on the right.

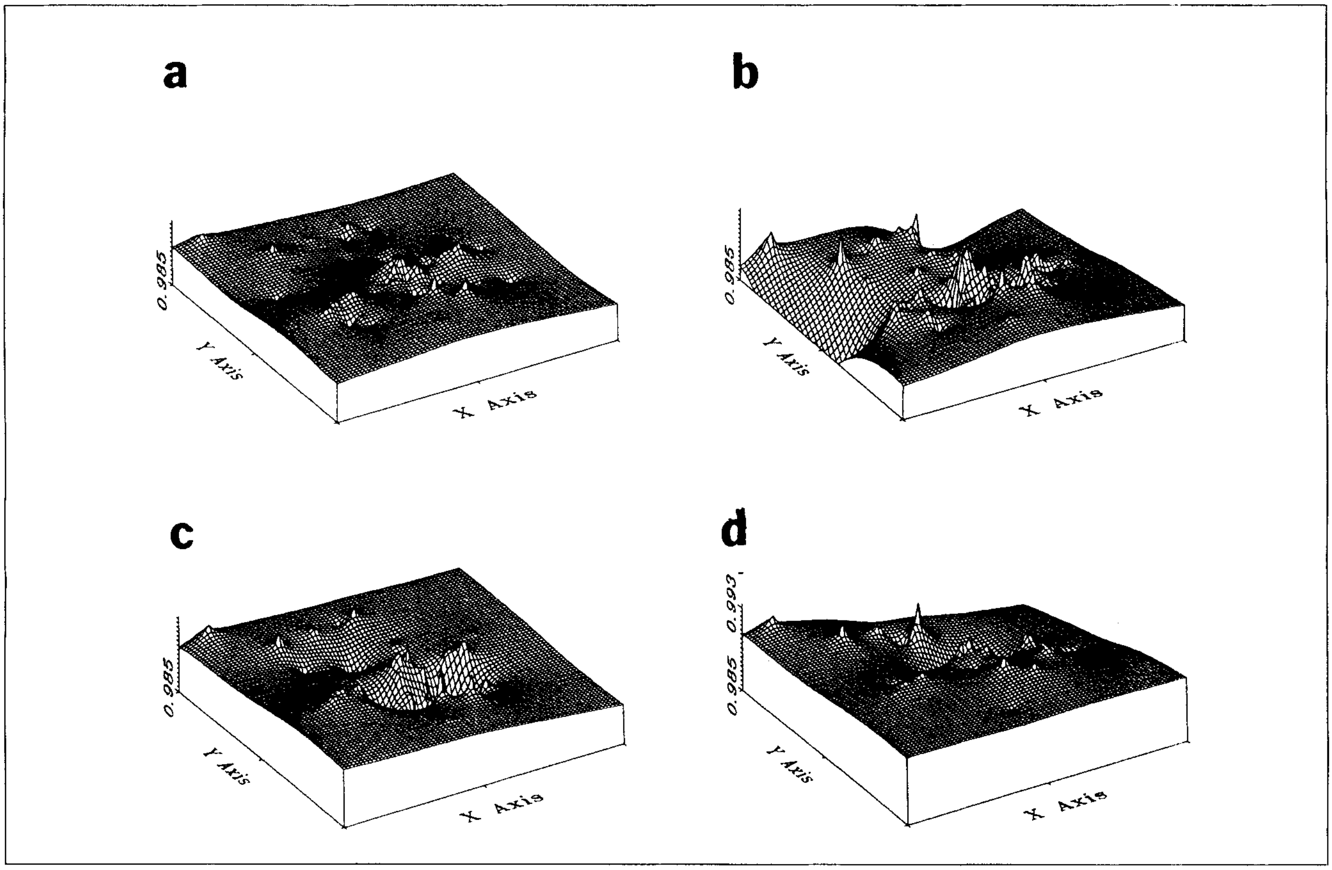

Figure 2. Evolution of the concentration field: area fraction ~0.

The initial distribution is given in (a) and the distributions at three successive times are given by the other three plots (c-d).

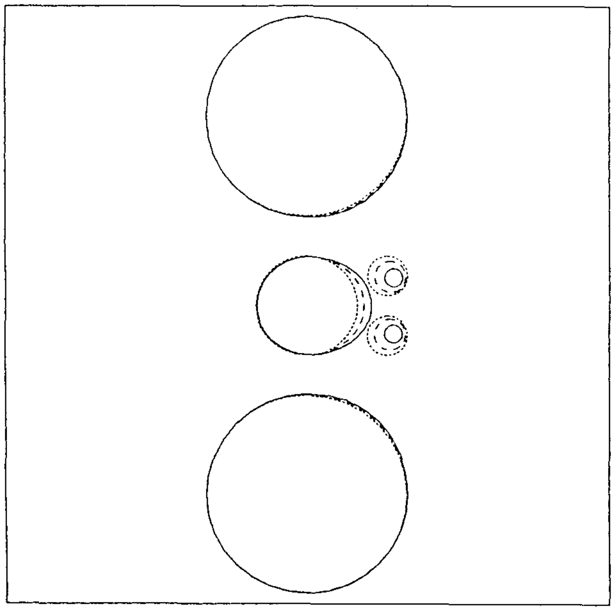

Figure 4. Evolution of a five-particle system.

. . . . , initial condition; - - - -, intermediate time; ———, final condition. The center particle shows a significant degree of deformation as it grows. The two smaller particles to the right remain circular as they shrink. As a result of the uneven growth rates, the center of mass of these smaller particles is not stationary, leading to the alteration of the local particle density.

Glicksman, 1984b), since particle A grows and moves into the larger particle size category. The different behavior is caused entirely by the difference in the local environment felt by the individual particles. As described in the previous paragraph, a concentration gradient, in fact, extends from one particle to another so that particle A experiences an environment that consists of relatively small particles compared to itself, whereas the opposite is true for particle B. Therefore, as a general rule, *particles which find themselves close to very small particles will be more likely to grow.*

Particle shape evolution

Previous investigators commonly assumed that the particles remained spherical to simplify the formulation by using points to represent particles. While this simplifies the problem, it is unclear whether such approximations overlook some of the more subtle aspects of the problem, such as particle deformation, apparent particle motion, and the effect of local anisotropic growth. To study these effects, we carried out a simulation, whose results are shown in Figure 4, with only five initially circular particles, each of which is discretized using 32 points. This system was chosen to exaggerate each of the effects and, at the same time, provide high resolution so that these effects would not be masked. As the system evolves, the initially circular center particle deforms, as a result of the increased growth rate in the direction facing the smaller particles. It should be pointed out that there is no anisotropy in this system so that the preferred equilibrium particle shape is circular. This simulation, therefore, shows that particle deformation is quite possible even for isotropic systems if the particle concentration is high enough. The controlling factor in this behavior is the balance between relaxation and growth, or the competition between two length scales—the capillary length and the interparticle separation. For systems with sufficiently low particle concentration, the mass flux through the interparticle matrix is small with respect to the redistribution of material within a particle, so the particles will remain mostly circular. The particle concentration at which this transition occurs is, therefore, a function of the surface tension. Finally, this observation underscores the disadvantage of representing particles as points and the importance of incorporating the flexibility of variable shape. These conclusions are in general in accord with similar calculations by Voorhees et al. (1988).

Apparent particle motion

Besides showing the phenomenon of particle deformation, the simulation shown in Figure 4 also demonstrates apparent particle motion. Note that as the two smaller particles shrink, their centers of mass also appear to move away from the center particle. This is again due to the uneven growth rate of the surface of these particles, since that part of the surface facing the larger particle shrinks faster than the rest. Unlike the center particle which deforms, these two particles remain circular. This is because these particles have higher curvature than the center particle so that the relaxation (restoration) effect of surface tension is greater. Apparent motion, therefore, alters the local environment which again cannot be accounted for by methods that treat the particles as points. Once again, this behavior is more important for systems with high volume fractions, since the change in separation can be of the order of the separation itself.

Particle-size distribution

The classical analytical theories provide a mathematical proof (Lifshitz and Slyovoz, 1961) that the normalized PSD approaches an asymptotic form for long times. While we have shown that the ordering of the particles is not preserved, the PSD in our simulations did approach an asymptotic form as demonstrated by the evolution of its dimensionless standard deviation. Figure 5 shows the development of the normalized standard deviation (standard deviation divided by mean) of the PSD with time. The standard deviation initially increases with time and eventually reaches a constant value more or less. The initial increase shows the spreading out of the initially sharp PSD, while the fluctuations are due to small system effects. It is very interesting to note that even though the basis on which the analytical theories were built is not quite correct, the macroscopic behavior is crudely described. It should also be noted that the shrinkage order is still not preserved at any stage, irrespective of the shape of the PSD. The fact that a constant value is reached in each case indicates that the PSD has attained a steady-state "self-preserving," shape which is consistent with experiments as well as theory. Due to the small system effects in our simulations, however, it is not easy to interpret the relationship between the width of the PSD and the particle concentration. Further simulations with greater numbers of particles may help elucidate this point.

One of the goals of this kind of study is to obtain the coarsening rate constant. A more demanding test is the PSD, however, since other quantities can be derived from the PSD. In each of the PSD evolution plots, Figures 6a to 6d, PSD's

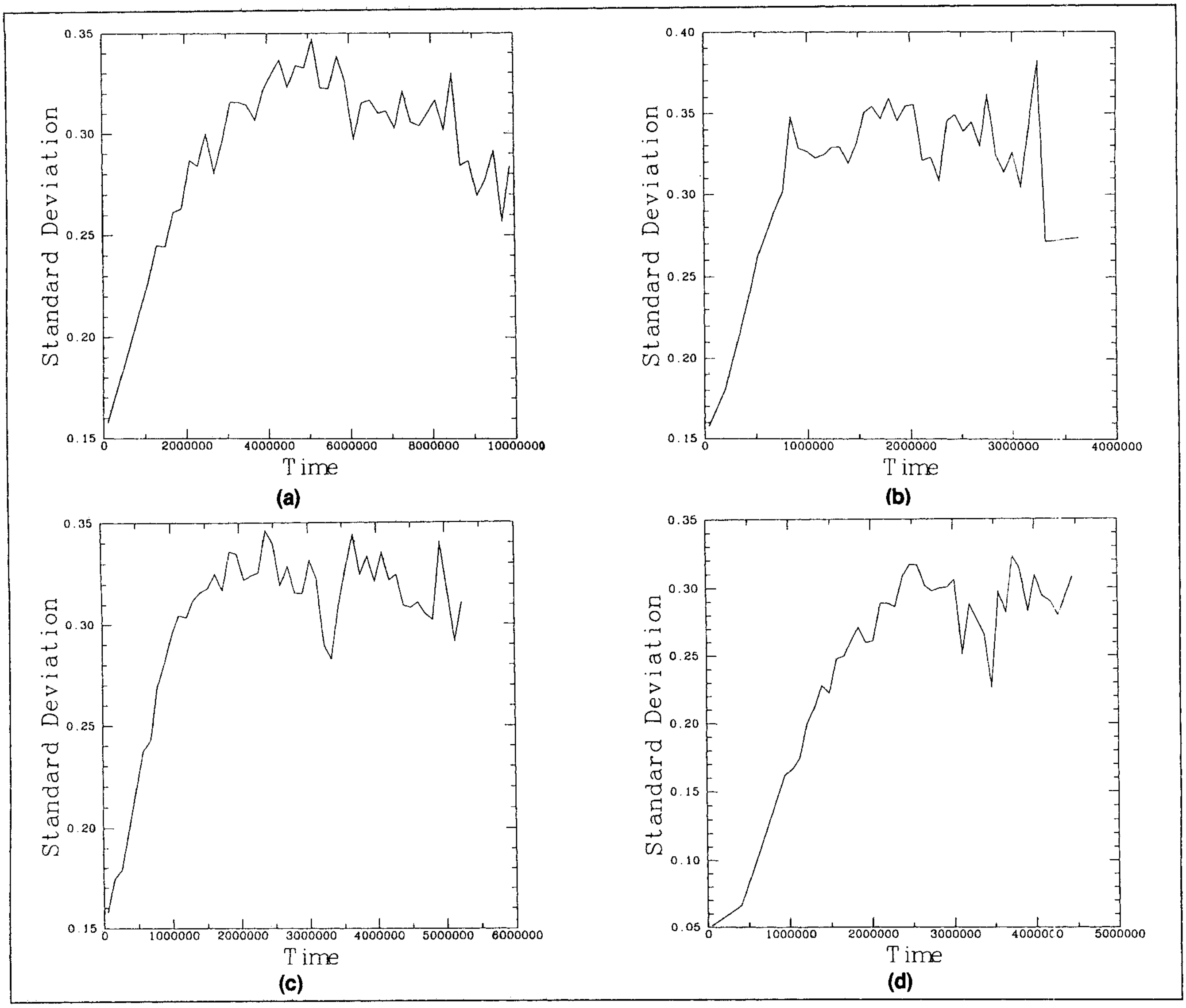

Figure 5. Evolution of the standard deviation of the PSD.

Area fraction = a, ~0; b, 0.06; c, 0.15; d, 0.213. β = a, 0; b, 0; c, 0; d, 100.

at three successive times are shown: initial (dot), intermediate (dash), and final steady state (dash-dot). The solid curve represents the two-dimensional version of the LSW theory (Hillert, 1965). Despite the apparent difference between our model and the LSW theory, our model (Figure 6a) reproduced the two-dimensional LSW-PSD result in the low particle concentration limit. It is a good indication that our method is at least correct in this limit and likely to be correct at other values as well. The agreement at low particle concentration is likely to be a result of the cancellation occurring in the system: the variations in the local environment are averaged out in the ensemble-averaging step so that the net effect is similar to the simplified assumption used in theories. As the particle concentration is raised, the shape of the PSD begins to deviate from that of the theory. The deviation is small, however, at low particle concentration (~6% in Figure 6b). The deviation is more significant at higher concentration (~15% in Figure 6c) with the final steady-state PSD being more symmetric, in a trend similar to that observed experimentally. Similar observations have also been reported by Voorhees and Glicksman.

Even though the deviation is small for an equilibrium system ($\beta = 0$) at 6% area fraction, a more symmetric PSD is obtained when β is set to 100 for a similar area fraction (Figure 6d): the system is no longer diffusion-limited, but local reaction limitation can also occur. This more symmetric PSD is caused by slowing down the shrinkage rate of the small particles. Thus, particles that otherwise would become smaller remain as larger particles, resulting in a more symmetric PSD. In other words, while the whole system remains mostly diffusion-limited, reaction limitation can happen, particularly to smaller particles, yielding a more symmetric PSD. By the same token, the particle removal rate is also reduced. The neglect of this effect in the analytical theories may well be a major contributor to their failure to agree with experiment.

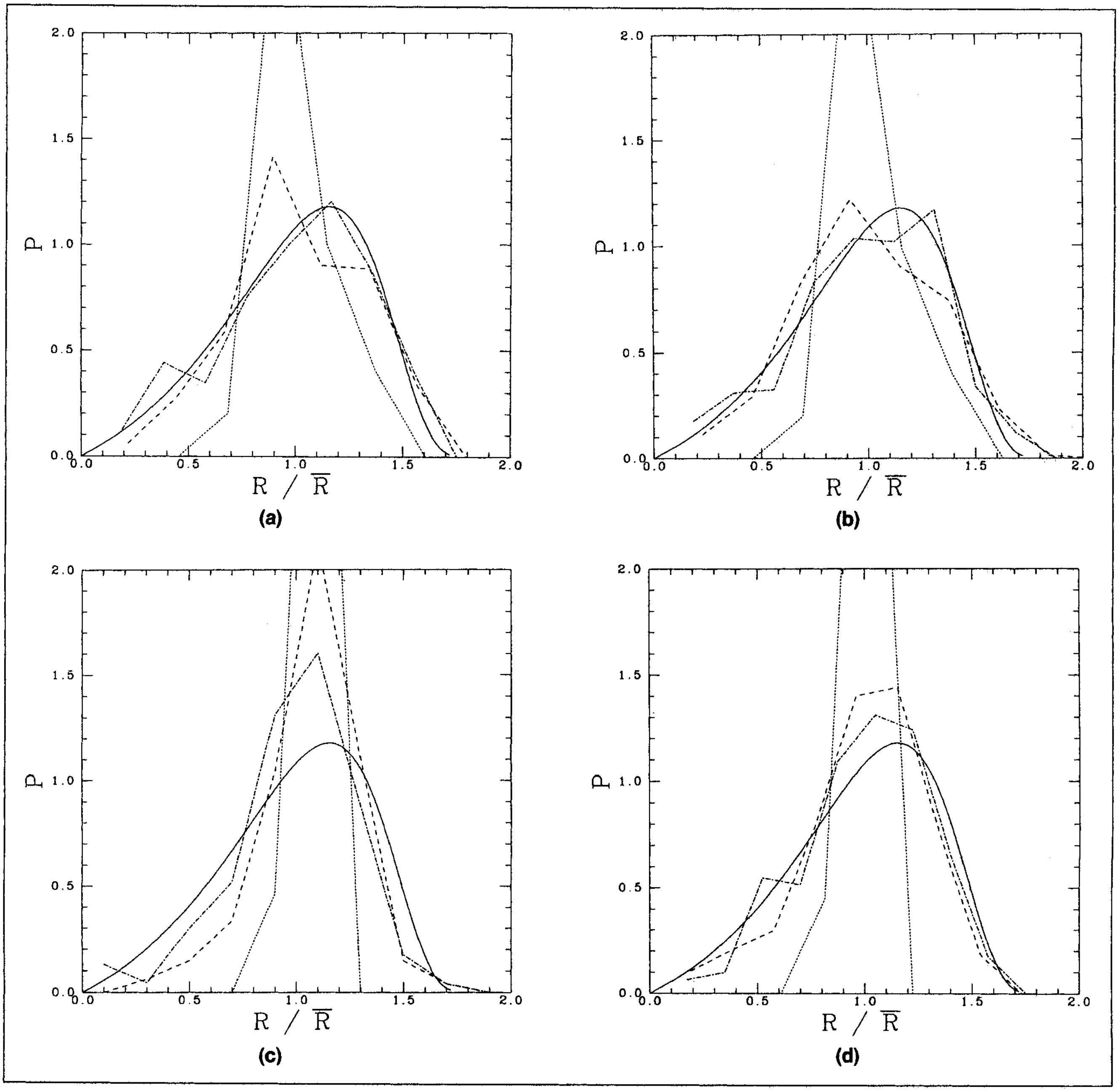

(a) (b) (c) (d)

Figure 6. Evolution of an ensemble-averaged particle-size distribution.

. . . . , initial distribution; - - - -, intermediate time; - · - ·, final time.

Area fraction = a, ~0; b, 0.06; c, 0.15; d, 0.07. β = a, 0; b, 0; c, 0; d, 100.

In each case, the smooth solid curve represents the LSW theory for two dimensions.

Volume fraction effects

Figure 7 shows ensemble-averaged variations of average particle size with time for several of our simulations; the slope at later times of each of these lines is related to the coarsening rate constant. The slopes are synopsized in the form of normalized coarsening rate constants in Figure 8. Each line on Figure 8 presents the coarsening rate constant (normalized by its value at vanishing area fraction) as a function of area fraction for a different value of β. Note that the coarsening rate constant appears to be insensitive to β, despite the fact that β was shown above to influence the *shape* of the PSD.

While we have few data points, and there is quite an amount of uncertainty in the numbers that we have obtained, it is possible that the coarsening rate constant is not a monotonic function of the particle concentration. These preliminary results appear to support a maximum in the rate constant variation with volume fraction. Although the existence of a local maximum has never been reported, we note that an inflection point has been reported (Jayanth and Nash, 1989). The present

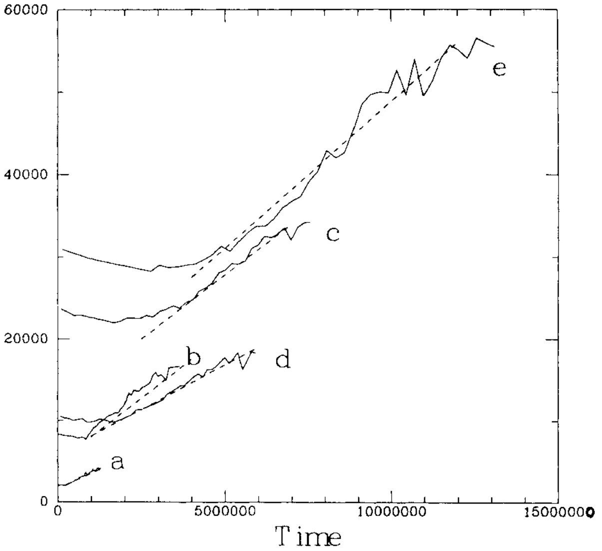

Figure 7. Evolution of the coarsening rate constant.

Area fraction = a, ~0; b, 0.061; c, 0.15; d, 0.07; e, 0.21. β = a, 0; b, 0; c, 0; d, 100; e, 100.

Curve a corresponds to the LSW limit. The coarsening rate constant for each case is obtained from the slope at later times after the initial "flat" region. The initial region is due to the spreading-out of the initially narrow PSD.

observation may be an artifact of our two-dimensional system. The relative insensitivity of the coarsening rate constant to the particle concentration (variations of no more than a factor of 2 for the area fraction range considered here) may be explained by noting that the rate constant is derived from the PSD. As discussed earlier, the PSD becomes more symmetric when the particle concentration is raised; hence, the associated rate constant also becomes slower than that if the shape of the PSD remain unchanged (since the rate constant is associated with the *average* particle size). Furthermore, it should be noted that the shape of the particles differs significantly from spherical at high particle concentration so that the analytical theories are not strictly applicable. At lower volume fractions, on the other hand, the variations in the rate constant are small enough to be masked by experimental errors.

For each of the cases shown in Figure 7, note that there is an initial period where the average particle size remains constant more or less. This is a direct consequence of the narrow PSD used initially. The PSD spreads out on both sides, resulting in a relatively stable average particle size. Due to the conservation of mass (area), the tail (smaller particles) develops faster than the head (larger particles), yielding a skewed PSD. The spreading of the initially sharp PSD implies that a narrow PSD is unstable and it tends to broaden.

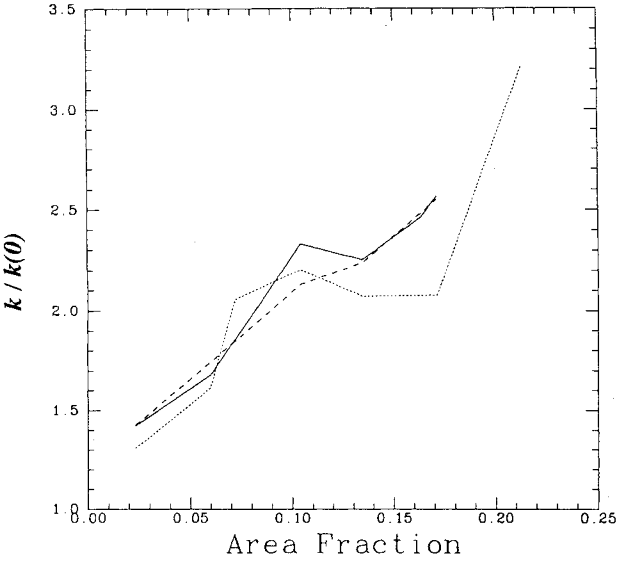

Figure 8. Variation of the normalized coarsening rate constant, $k(\varphi)/k(0)$, with area fraction φ.

———, $\beta = 0$; - - - -, $\beta = 10$; . . . ., $\beta = 100$.

Performance of simulation method

The generality of our method does not come without cost; the size of the system we may study (the number of particles and the number of discretization points per particle) is limited. The current program can readily handle 65 particles with eight discretization points per particle. The average run time on the Cray Y-MP at the Pittsburgh Supercomputing Center is approximately 30 minutes with a performance rating of 147 MFLOPS, which is a result of our highly vectorized code. While the effort involved is by no means trivial (approximately 700 first-order stiff nonlinear ordinary differential equations, each of whose driving functions is the solution to an integral equation), the number of particles is still small compared to similar work. Nonetheless, we believe that the potential for increasing the number of particles to be studied is great. Because of the nature of the problem, parallelization should yield great dividends. The latter can be understood by noting that vectorization in general improves the performance of the innermost loops of a computation, while parallelization deals with the outermost loops. Hence, a number of the computational stages could be performed concurrently, resulting not only in shorter run times but also in better utilization of the computer. This will be implemented at a later stage. Further refinement might include the introduction of a "screening length" to restrict the bandwidth of the Green's function matrix.

Conclusions

A method for describing two-dimensional diffusion-limited coarsening was presented. The method can handle virtually any volume fraction; hence, it transcends the usual small volume fraction limit. It was demonstrated that the mean-field approximation is statistically, rather than locally, valid even in the limit of small volume fraction. Furthermore, the order of the growth or shrinkage of the particles was found to be violated in disagreement with the usual theories. The ensemble-averaged coarsening behavior, in contrast with experimental findings, depends slightly on the volume fraction.

In spite of these differences, the ensemble-averaged behavior was found to conform reasonably well with existing theories ($\overline{R}^2 \propto t$) based on mean-field theory. The agreement was attributed to the cancellation effects caused by the random nature of the local environment (the "microstructural noise" mentioned by Voorhees and Glicksman). While the coarsening process obeys the mean-field functional behavior, the PSD does not have the shape predicted by the mean-field approach. A narrow PSD was shown to be unstable, and the standard deviation (and hence the shape) of the steady-state PSD qualitatively was found to be insensitive to the volume fraction. Local "reaction" or mass transport limitation can occur for small particles, causing them to decay more slowly and leading to a more symmetric PSD.

Acknowledgment

This work was supported in part by the National Science Foundation through Research Initiation Award CBT-8809548. The authors wish to express their gratitude to the Pittsburgh Supercomputing Center, where most of the numerical simulations were performed, for its support through grant CBT-8900012P. We acknowledge the inspiration of Prof. R. T. DeHoff of the University of Florida whose recent seminar at Yale prompted us to undertake this investigation.

Notation

B = ratio of the diffusivities (Eq. 8)
c = concentration
D = diffusion coefficient
ds_i' = differential arclength along a cluster interface ($i=1, \ldots, N$)
G = Green's function
j = mass flux
k = coarsening rate constant (Eq. 4)
k_m = mass transfer coefficient
K = diffusivity
$\hat{n}$ = outward unit normal
N = number of clusters
P = probability density function for reduced area
r = radial position
R_g = universal gas constant
R_∞ = radius of the outer boundary
S_i = cluster interface ($i=1, \ldots, N$)
S_T = total arclength of cluster
t = time
T = temperature
v = normal velocity
x = reduced supersaturation
X = location of the source (field) point
Y = location of the field (source) point

Greek letters

α = relative arclength
ϕ = dimensionless field variable
ϕ_n = normal derivative of ϕ
φ = area fraction
ρ = density
γ = surface energy
Γ = capillary length
κ = local curvature
θ = angle between the normal and y-axis

Literature Cited

Ardell, A. J., "The Effects of Volume Fraction on Particle Coarsening: Theoretical Considerations," *Met. Trans.*, **1**, 525 (1970).

Brower, R. C., D. A. Kessler, J. Koplik, and H. Levine, "Geometrical Models of Interface Evolution," *Phys. Rev.*, **A29**, 1335 (1984).

Chakraverty, B. K., "Grain Size Distribution in Thin Films," *Phys. Chem. Solids*, **28**, 2401 (1967).

Chellman, D. J., and A. J. Ardell, "The Coarsening of γ' Precipitates at Large Volume Fractions," *Acta Metall.*, **22**, 577 (1974).

Dadyburjor, D. B., S. P. Marsh, and M. E. Glicksman, "The Role of Multiparticle-Adatom Interactions on the Sintering of Supported Metal Catalysts," *J. Catal.*, **99**, 358 (1986).

Dettman, J. W., *Mathematical Methods in Physics and Engineering*, Dover, New York (1988).

Doherty, R. D., "Nucleation of Recrystallization in Single Phase and Dispersion Hardened Polycrystalline Materials," *Metal. Sci.*, **16**, 1 (1982).

Dritschel, D. G., "Contour Dynamics and Contour Surgery: Numerical Algorithms for Extended, High-Resolution Modelling of Vortex Dynamics in Two-Dimensional, Inviscid, Incompressible Flows," *Comp. Phys. Rep.*, **10**, 77 (1989).

Enomoto, Y., K. Kawasaki, and M. Tokuyama, "Computer Modeling of the Growth Kinetics of Leged Interphase Boundaries: II. Finite Train of Steps," *Acta Metall.*, **35**, 907 (1987).

Fischmeister, H., and C. Grimvall, "Sintering and Related Phenomena," *Materials Science Research*, G. C. Kuczynski, ed., **6**, Plenum Press, New York (1973).

Greenwood, G. W., "The Growth of Dispersed Precipitates in Solutions," *Acta Metall.*, **4**, 243 (1956).

Hillert, M., "On the Theory of Normal and Abnormal Grain Growth," *Acta Metall.*, **13**, 227 (1965).

Jayanth, C. S., and Philip Nash, "Review. Factors Affecting Particle-Coarsening Kinetics and Size Distribution," *J. Mat. Sci.*, **24**, 3041 (1989).

Langer, J. S., "Instabilities and Pattern Formation in Crystal Growth," *Rev. Mod. Phys.*, **52**, 1 (1980).

Lifshitz, L. M., and V. V. Slyozov, "The Kinetics of Precipitation from Supersaturated Solid Solutions," *J. Phys. Chem. Solids*, **19**, 35 (1961).

Marqusee, J. A., and J. Ross, "Theory of Ostwald Ripening: Competitive Growth and Its Dependence on Volume Fraction," *J. Chem. Phys.*, **80**, 536 (1984).

McFadden, G. B., P. W. Voorhees, R. F. Boisvert, and D. I. Meiron, "A Boundary Integral Method for the Simulation of Two-Dimensional Particle Coarsening," *J. Scientific Computing*, **1**, 117 (1986).

Petzold, L. R., "Automatic Selection of Methods for Solving Stiff and Nonstiff Systems of Ordinary Differential Equations," *SIAM J. Sci. Stat. Comput.* **4**, 136 (1983).

Voorhees, P. W., and M.E. Glicksman, "Solution of the Multi-Particle Diffusion Problem with Application to Ostwald Ripening: I. Theory," *Acta Metall.*, **32**, 2001 (1984a).

Voorhees, P. W., and M. E. Glicksman, "Solution of the Multi-Particle Diffusion Problem with Application to Ostwald Ripening: II. Computer Simulations," *Acta Metall.*, **32**, 2013 (1984b).

Voorhees, P. W., G. B. McFadden, R. F. Boisvert, and D. I. Meiron, "Numerical Simulation of Morphological Development during Ostwald Ripening," *Acta Metall.*, **36**, 207 (1988).

Wagner, C., "Theorie der Alterung von Niederschlägen durch Umlösen," *Z. Electrochem.*, **65**, 581 (1961).

Wong, T. H., "Two-Dimensional Studies of Cluster Interface Dynamics," PhD Diss., Yale University (1991).

Wong, T. H., and J. A. O'Brien, "Effects of Growth Mechanisms on Cluster Morphology Studied by Contour Dynamics," *Phys. Rev.*, **A41**, 4439 (1990).

Appendix: Interface Reaction Limitation

It is commonly assumed that local equilibrium exists at the interface between particles and their surroundings: the rate of the kinetic processes at the surface of the particle is fast with respect to diffusion so that the kinetics of the interface reaction can be ignored. This assumption is quite reasonable for larger particles because their growth rates are generally smaller than those of the shrinking particles. This is a direct result of the constraint of material conservation. Consider a system consisting of only two unequally sized particles. The relationship between the sizes as they exchange material can be trivially shown to be

$$\frac{dR_1}{dR_2} = -\frac{R_2}{R_1} \tag{A1}$$

If one particle is ten times smaller than the other, it shrinks ten times faster. A similar argument also applies to an ensemble of particles. It is, therefore, quite possible for the rate of "reaction" to become a factor in determining the shrinkage rate of smaller particles. It would, therefore, be useful to estimate the onset of reaction limitation. A simple approach is to pick a typical value of the coarsening rate constant from experiment. For the Ni-Al system at 800°C, the coarsening rate constant $k \sim 10^{-21}\text{cm}^3/\text{s}$ (Chellman and Ardell, 1974), which is $\propto d\bar{R}/dt$. The dimensionless velocity can be expressed as:

$$v = \left(\frac{k}{3\bar{R}^2}\right) \bigg/ \left(\frac{R_{\text{ref}}}{t_{\text{ref}}}\right), \tag{A2}$$

where we picked the reference length scale of the system to be 10^{-8}cm in our simulations, $\bar{R} \sim 10^{-6}$cm, and t_{ref} is the reference time given by:

$$t_{\text{ref}} = \frac{\Gamma^2}{DC_\infty v_m}. \tag{A3}$$

For many materials, the reciprocal of the molar volume v_m, which has the unit of inverse concentration, is likely to have the same order as C_∞, the concentration at the boundary of the system, such that the product $C_\infty v_m$ would be of order unity. The capillary length Γ is of order 10^{-7}cm (Voorhees and Glicksman, 1984) and $D \sim 10^{-12}\text{cm}^2/\text{s}$ (Chellman and Ardell, 1974). With this set of parameters, the dimensionless velocity $v \approx 3 \times 10^{-4}$. This is a lower bound because it is estimated from the growth rate of an "average" particle, and the interface velocity of small particles is likely to be one or two orders of magnitude higher. Nevertheless, it shows that reaction limitation could become significant at some reasonable dimensionless velocity.

As shown by Wong and O'Brien (1990), if deviation from local equilibrium is small, reaction limitation can be incorporated into our model as follows:

$$\phi = 1 - \Gamma\kappa - \beta v, \tag{A4}$$

where β is the kinetic parameter given by

$$\beta = \frac{\rho D}{k_m \Gamma \Delta c}. \tag{A5}$$

Again using the above coarsening rate constant, $k_m \Delta c$ is estimated to be $\sim 10^{-7}\ \text{g/cm}^2\cdot\text{s}$ and the density of these materials $\rho \sim 2\ \text{g/cm}^3$. With these parameters, the corresponding value of β is 200. This is only an estimate, and its value may in fact vary considerably; hence, we (conservatively) chose β to be 100 in some of the simulations to assess the effect of reaction limitation on the dynamics of coarsening.

Manuscript received Jan. 23, 1991, and revision received May 23, 1991.